Combining Switched TMAs and FDAs to Synthesize Dot-Shaped Beampatterns

Roberto Maneiro-Catoira, *Member, IEEE,* Julio Brégains, *Senior Member, IEEE,*
José A. García-Naya, *Senior Member, IEEE,* and Luis Castedo, *Senior Member, IEEE*

***Abstract*—The application of frequency offsets to the elements of a conventional phased array with variable phase shifters (VPSs) leads to frequency diverse arrays (FDAs) with the ability to provide range-angle spatial focusing. In this letter, we propose an innovative approach to FDA using switched time-modulated arrays (TMAs) instead of VPSs. The time modulation efficiency of the combined FDA-TMA approach is over 94% when using Kaiser windows to determine the frequency offsets. Such windows have the advantage of flexibly handling the trade-off between the beam collection efficiency and the half power beamwidth without the need of difficult optimizations.**

***Index Terms*—Frequency Diverse Arrays, Time-modulated arrays.**

I. Introduction

FREQUENCY Diverse Arrays (FDAs) apply frequency offsets to the elements of an antenna array to generate radiation patterns which in general depend on the angular variables φ and θ, the distance (range) r, and the time t [1]–[3]. Progressive incremental frequency offsets cause FDAs to generate time-variant power radiation patterns with periodic spatial multiple maxima [2]. This property has the disadvantage of radiating signals over non-desired maxima which interfere with the desired signal. To avoid this range-angle periodicity, different alternatives have been considered such as non uniform frequency offsets [4]–[8] or time-modulated frequency offsets [9]–[12]. These two methods allow for the synthesis of s- and dot-shaped diagrams with a single maximum in the range-angle space. To support this feature, each antenna element in the array uses a variable phase shifter (VPS) to provide an additional phase term that allows for the spatial steering of the FDA. Nevertheless, such a single maximum is not static in time [13], [14].

In this letter, we propose an innovative FDA architecture that combines non-uniform Kaiser window-based frequency offsets with efficient and versatile switched time-modulated arrays (TMAs). While the former allows for the selection of the range-angle coordinates and guarantees a fine focusing without optimization, the latter exploits the first positive harmonic and provides the corresponding adaptive weights to focus on such coordinates without using VPSs. Additionally, the time-variant maximum issue is overcome by imposing a restriction involving the transmitted pulsed signal period and the maximum frequency offset employed. This allows for the generation of a quasi-static dot shaped beam pattern. These features make the proposed FDA approach well suited for those long-range applications where mitigation of range-dependent interferences is fundamental (e.g., secure communications).

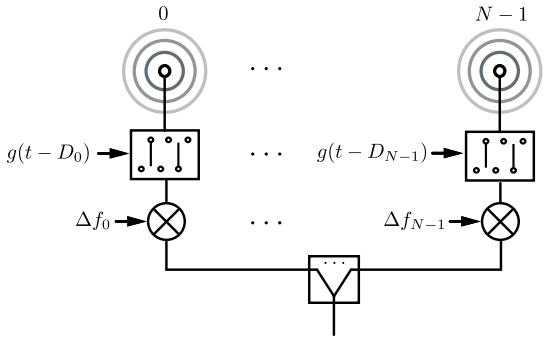

Fig. 1. The proposed combined FDA-TMA antenna array feeding network.

II. Signal model

Let us consider a uniformly excited N-element antenna array equipped with the combined FDA-TMA feeding network shown in Fig. 1. If the array transmits a single-frequency signal of the form $e^{j2\pi f_c t}$, being f_c the carrier frequency, the FDA part of the feeding network produces the frequency-shifted signals $e^{j2\pi f_n t}$, $n{=}0,\ldots,N{-}1$, where $f_n{=}f_c+\Delta f_n$, being Δf_n the frequency offset applied at the n-th antenna element. For the sake of simplicity, we assume that $\Delta f_0{=}0$. Next, signals are time modulated by a set of multilevel periodic pulsed waveforms $h_n(t)$, $n{=}0,\ldots,N{-}1$, to produce the transmitted signals

$$s_n(t) = h_n(t)\mathrm{e}^{\mathrm{j}2\pi f_n t}, \quad n=0,\ldots,N-1. \tag{1}$$

All time modulating signals $h_n(t)$ have the same fundamental period T_μ and fundamental frequency $f_\mu{=}1/T_\mu$. The constraint $f_\mu{\ll}f_c$, is imposed to avoid spectral signal overlapping [16].

Fig. 2 explains how $h_n(t)$ are readily synthesized from SPDT switches. The starting point is the construction of the four-level basic periodic pulsed waveform $p(t)$ shown in Fig. 2a as the sum of three periodic bipolar square pulses that have a certain fixed time delay between them [15]. Time

* Corresponding author: José A. García-Naya (jagarcia@udc.es).

This work has been funded by the Xunta de Galicia (by grant ED431C 2020/15, and grant ED431G 2019/01 to support the Centro de Investigación de Galicia "CITIC"), the Agencia Estatal de Investigación of Spain (by grants RED2018-102668-T and PID2019-104958RB-C42) and ERDF funds of the EU (FEDER Galicia 2014-2020 & AEI/FEDER Programs, UE)

CITIC Research Center, University of A Coruña, 15071 A Coruña, Spain. E-mail: roberto.maneiro@udc.es, julio.bregains@udc.es, jagarcia@udc.es, luis@udc.es.

Digital Object Identifier

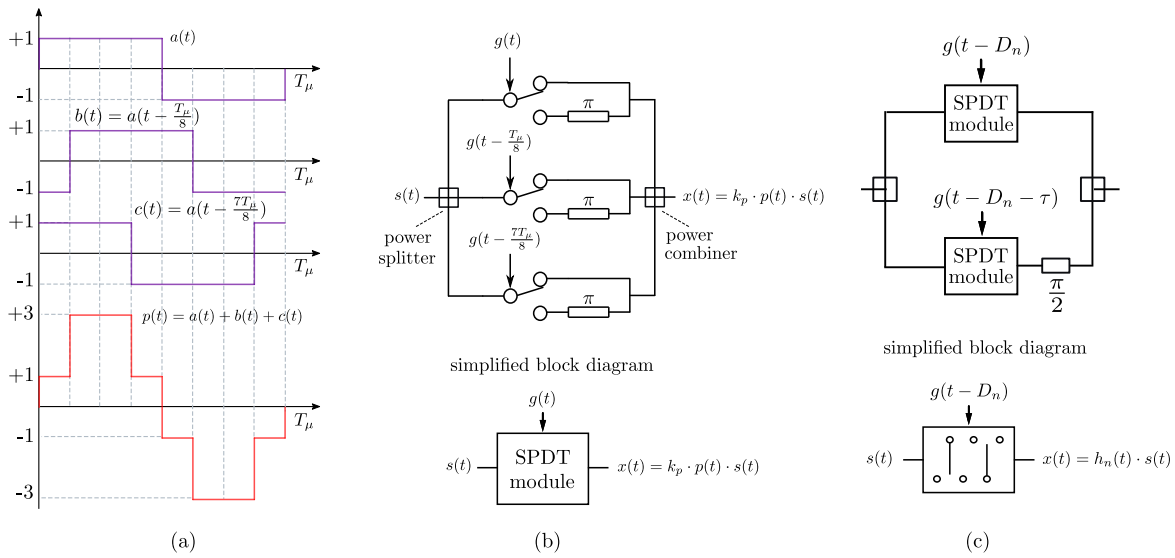

Fig. 2. (a) Synthesis of the stair-step approximation of a sine function $p(t)$ as the sum of delayed bipolar squared sequences; (b) SPDT switches connection to time modulate with $p(t)$ and its simplified representation termed SPDT module. The unipolar signal that controls the switches is $g(t) = 1$ if $a(t) \geq 0$ and $g(t) = 0$ if $a(t) < 0$; (c) SSB TMA feeding network built with two SPDT modules and its corresponding block representation. Although it shows higher complexity than standard phased arrays, it exhibits a higher phase resolution response and an excellent competitive advantage in cost [15].

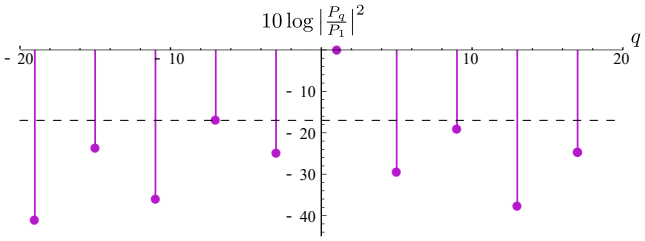

Fig. 3. Normalized Fourier series spectrum (in dB) of $h_n(t)$ (see (3)). The largest secondary component is $q = -7$ and its relative level -16.9 dB is emphasized with a dashed line.

modulating with $p(t)$ is efficiently implemented with the SPDT switches connection shown in Fig. 2b where the switches are controlled by delayed versions of the same unipolar squared pulse $g(t)$. At the output of the SPDT module in Fig. 2b we have the signal $x(t)=k_p p(t)s(t)$, with $s(t)$ being the input signal and $k_p^2 = 1/5$ a normalizing constant resulting from matching the powers of $s(t)$ and $x(t)$ because ideal SPDT switches do not waste power since they have no off-state [15].

Finally, two SPDT modules are connected as in Fig. 2c to produce the n-th element TMA part of the proposed feeding network. This latter connection aims at removing the frequency-mirrored harmonics arising in conventional TMAs. The resulting time modulating signals are thus given by

$$h_n(t) = \frac{k_p}{\sqrt{2}} \left[p(t - D_n) + \mathrm{j} p(t - D_n - \tau) \right], \tag{2}$$

where D_n and $\tau = 1/(4f_\mu)$ are a variable and a fixed time delay, respectively [17]. Hence, identical signals with different delays govern the array elements.

Recall that $h_n(t)$ are periodic signals with fundamental period $f_\mu = 1/T_\mu$. Therefore, they can be represented by their exponential Fourier series expansions which, considering that $\mathrm{e}^{-\mathrm{j}q2\pi f_\mu \tau} = (-\mathrm{j})^q$, are readily obtained as

$$\begin{aligned} h_n(t) &= \frac{k_p}{\sqrt{2}} \sum_{q \text{ odd}} \left[1 - (-\mathrm{j})^{q+1} \right] P_q \mathrm{e}^{-\mathrm{j}q2\pi f_\mu D_n} \mathrm{e}^{\mathrm{j}q2\pi f_\mu t} = \\ &= \sqrt{2} k_p \sum_{q \in \Xi} P_q \mathrm{e}^{-\mathrm{j}q2\pi f_\mu D_n} \mathrm{e}^{\mathrm{j}q2\pi f_\mu t}, \end{aligned} \tag{3}$$

where

$$P_q = \frac{1}{\mathrm{j}\pi q} \left[2 - 2\sqrt{2} \cdot (-1)^{\frac{(q+3)(q+5)}{8}} \right] \tag{4}$$

are the Fourier series coefficients of $p(t)$ and $\Xi = \{q = 4k - 3; k \in \mathbb{Z}\} = \{\dots, -7, -3, 1, 5, \dots\}$ is the set of indexes of the non-zero harmonics [15]. We now introduce the TMA dynamic excitations as

$$I_{nq} = \sqrt{2} k_p P_q \mathrm{e}^{-\mathrm{j}q2\pi f_\mu D_n} \tag{5}$$

which allows us to rewrite equation (3) as

$$h_n(t) = \sum\nolimits_{q \in \Xi} I_{nq} \mathrm{e}^{\mathrm{j}q2\pi f_\mu t}. \tag{6}$$

In view of (5), the moduli of the dynamic excitations $|I_{nq}| = \sqrt{2} k_p P_q$ do not depend on n, whereas the phases ϕ_{nq} depend on qD_n. Hence, the power radiation pattern of any harmonic corresponds to that of a uniform linear array and can be readily steered by properly adapting the phase terms qD_n. Fig. 3 shows the normalized Fourier series mean square spectrum of $h_n(t)$ where we can observe that the most meaningful harmonic is $q = 1$ with a relative peak level of at least 16.9 dB above the remaining ones. Hence, such a harmonic, located at $f_c + f_\mu$, will be the exploited one.

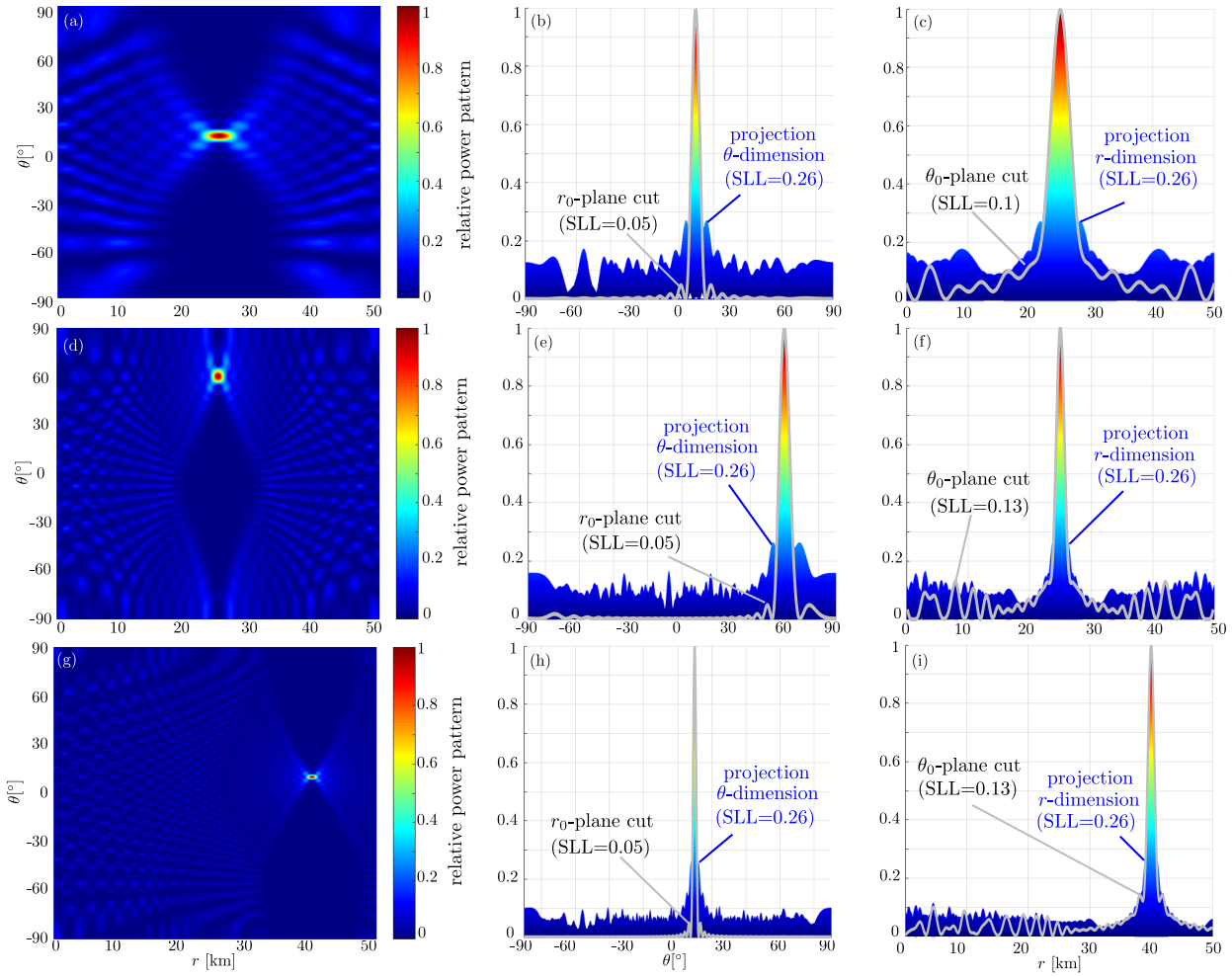

Fig. 4. Projection of the transmit quasi-static spatial focusing beampatterns of the proposed FDA-TMA approach on the range-angle dimensions, angle dimension and range dimension, and r_0-plane and θ_0-plane cuts (in grey), for three different spatial locations of the target and considering different number of antenna elements N: (a)(b)(c) N=19, (r_0,θ_0)=(25 km, 10°), α = 1.08; Δf=150 kHz; HPBW$_r$=4.1 km; HPBW$_\theta$=5.5°; (d)(e)(f) N=29, (r_0,θ_0)=(25 km, 60°), α=1.52; Δf=150 kHz; HPBW$_r$=1.76 km; HPBW$_\theta$=3.0° (g)(h)(i) N=49, (r_0,θ_0)=(40 km, 10°), α=1.64; Δf=150 kHz; HPBW$_r$=1.30; HPBW$_\theta$=1.25°. Notice that the Kaiser windows (11) provide dot-shaped patterns with SLL values equal to 0.05 in the r_0-plane cut, 0.13 in the θ_0-plane cuts, and 0.26 in the whole range-angle sector Ω=$\{r \in (0\,\text{km}, 50\,\text{km}); \theta \in (-90°, 90°)\}$.

According to (1) and (6), the signal radiated at an arbitrary probe point having spatial coordinates $(r,\,\theta)$ is

$$\begin{aligned} S(t,r,\theta) &= \sum_{n=0}^{N-1} \frac{1}{r_n} s_n\left(t-\frac{r_n}{c}\right) = \\ &= \sum_{n=0}^{N-1} \frac{1}{r_n} \sum_{q\in\Xi} I_{nq} \mathrm{e}^{\mathrm{j}q2\pi f_\mu\left(t-\frac{r_n}{c}\right)} \mathrm{e}^{\mathrm{j}2\pi f_n\left(t-\frac{r_n}{c}\right)} \\ &= \sum_{q\in\Xi} \sum_{n=0}^{N-1} \frac{1}{r_n} |I_{nq}| \mathrm{e}^{\mathrm{j}\left[2\pi(f_n+qf_\mu)\left(t-\frac{r_n}{c}\right)+\phi_{nq}\right]} \end{aligned} \quad (7)$$

where c is the speed of light and $r_n \approx r - nd\sin\theta$ the distance between the nth element and the probe point. Finally, considering $f_n = f_c + \Delta f_n$ and $1/r_n \approx 1/r$, we arrive at

$$\begin{aligned} S(t,r,\theta) &= \frac{1}{r} \sum_{q\in\Xi} \mathrm{e}^{\mathrm{j}2\pi(f_c+qf_\mu)\left(t-\frac{r}{c}\right)} \cdot \\ &\cdot \sum_{n=0}^{N-1} |I_{nq}| \mathrm{e}^{\mathrm{j}\phi_{nq}} \mathrm{e}^{\mathrm{j}2\pi\left[\Delta f_n\left(t-\frac{r}{c}\right)+\frac{nf_c d\sin\theta}{c}+\frac{n\Delta f_n d\sin\theta}{c}\right]}. \end{aligned} \quad (8)$$

III. Beampattern Synthesis

Assuming $|\Delta f_n| < f_\mu \ll f_c$, the term $n\Delta f_n d\sin\theta/c$ in (8) can be neglected [9], [10] and, hence, (8) can be rewritten as

$$S(t,r,\theta) = \frac{1}{r} \sum_{q\in\Xi} \mathrm{e}^{\mathrm{j}2\pi(f_c+qf_\mu)\left(t-\frac{r}{c}\right)} F_q(t,r,\theta) \quad (9)$$

where

$$F_q(t,r,\theta) = \sum_{n=0}^{N-1} |I_{nq}| \mathrm{e}^{\mathrm{j}\phi_{nq}} \mathrm{e}^{\mathrm{j}2\pi\left[\Delta f_n\left(t-\frac{r}{c}\right)+\frac{nf_c d\sin\theta}{c}\right]} \quad (10)$$

is the array factor corresponding to the q-th harmonic. We now consider that the FDA frequency offsets have the form $\Delta f_n = \Delta f \cdot \Upsilon(n)$ where Δf is a fixed offset and

$$\Upsilon(n) = \frac{\beta_0}{\beta_0[\alpha]} \left[\alpha\sqrt{1-\left(\frac{2(n-\frac{N-1}{2})}{N-1}\right)^2}\right] \quad (11)$$

are the weights of a Kaiser window which, besides being a near-optimal window [18, Chapter 4], allows for readily

adjusting the trade-off between the spatial SLL and the half power beamwidth (HPBW) by means of the parameter α, with $\beta_0[.]$ being the modified Bessel function of the first kind and zero order. We will assume that N is odd so that the Kaiser window is symmetrical.

According to (10), steering the useful harmonic (q=1) beampattern towards a target point with spatial coordinates (r_0, θ_0) is feasible if $\phi_{n1}=2\pi/c[\Delta f_n r_0 - n d f_c \sin\theta_0]$ or, equivalently, if the time delays in (5) are set to $D_n=-\phi_{n1}/(2\pi f_\mu)$. In such a case, the array factor for q=1 takes the form

$$F_1(t,r,\theta)=\sum_{n=0}^{N-1}|I_{n1}|e^{j2\pi\left[\Delta f_n\left(t-\frac{r-r_0}{c}\right)+n f_c d\frac{\sin\theta-\sin\theta_0}{c}\right]}. \quad (12)$$

which has a single maximum in (r_0, θ_0). Additionally, by considering the time-dependent phase $\Phi_n(t)=2\pi[\Delta f_n(t-(r-r_0)/c)+n f_c d(\sin\theta-\sin\theta_0)/c]$, we observe that its maximum variation for $t\in[0,T_\mu]$ is $2\pi(N-1)(\Delta f_n)_{\max}T_\mu$ (see [19]). Hence, imposing the constraint

$$(N-1)(\Delta f_n)_{\max}\ll f_\mu \quad (13)$$

leads the beampattern to exhibit a quasi-static behavior and thus to be approximated as $F_1(r,\theta)\approx F_1(t=0,r,\theta)$. Notice that since f_μ is limited by the maximum speed of the switches, (13) imposes an upper limit on Δf_n and, hence the technique is restricted, at present, to long-range applications. On the other hand, if we define the whole range-angle operating area as $\Omega=\{(r,\theta)/r\in(r_{\min},r_{\max});\theta\in(-90°,90°)\}$, the time modulation radiation efficiency, η_{TM}, when $d=0.5c/f_c$ turns out to be (see a similar derivation in [15, Section II-D])

$$\eta_{\text{TM}}=\frac{\iint_{(r,\theta)\in\Omega}|F_1(r,\theta)|^2\sin\theta\,d\theta\,dr}{\sum_{q\in\Xi}\iint_{(r,\theta)\in\Omega}|F_q(r,\theta)|^2\sin\theta\,d\theta\,dr}=\frac{1}{N}\sum_{n=0}^{N-1}|I_{n1}|^2$$
$$=\frac{1}{N}N\frac{2}{5}\left(\frac{2+2\sqrt{2}}{\pi}\right)^2=0.945. \quad (14)$$

IV. Numerical Results

Fig. 4 plots the resulting beam patterns obtained with the proposed FDA-TMA approach for three different target positions and number of antenna elements in order to illustrate its spatial focusing capabilities. We considered f_c=10 GHz and f_μ=200 MHz for which the 2-5 ns RF switches in [20, Table III] can be used. By properly adjusting the switch-on delays D_n, the Kaiser window parameter α, and the FDA parameter Δf, dot-shaped beam patterns pointing towards the target coordinates (r_0, θ_0) were obtained. Such patterns have a SLL value equal to 0.05 in the r_0-plane cut, equal to 0.13 in the θ_0-plane cut, and equal to 0.26 in the whole area Ω. The caption of Fig. 4 also provides the resulting values of HPBW$_r$ and HPBW$_\theta$ in each scenario. It is apparent that the larger the N, the narrower the beamwidth in both dimensions.

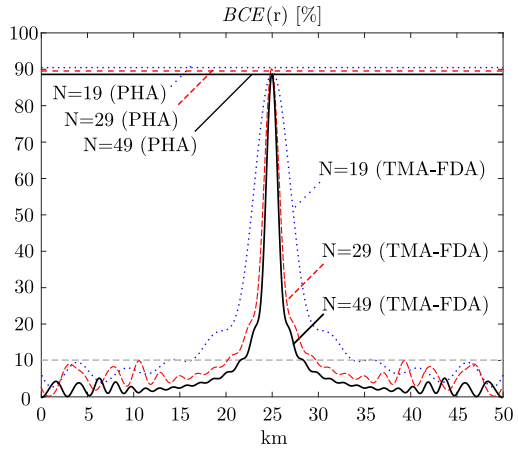

Fig. 5. BCE of the proposed FDA-TMA approach. The parameter α is set to ensure the BCE values to be below 10% outside the dot shaped beampatterns. For N=19 the accomplished target area is $\Psi(\Delta r{=}35\%,\Delta\theta{=}2.8\%)$, for N=29 is $\Psi(\Delta r{=}20\%,\Delta\theta{=}2\%)$ and for N=49, $\Psi(\Delta r{=}15\%,\Delta\theta{=}1.1\%)$. The comparison with conventional phased arrays, which exhibit a constant BCE value, is also shown.

The beam collection efficiency (BCE) is a helpful metric to assess the performance of FDAs [21] and is defined as

$$\text{BCE}(r)=100\cdot\frac{\int_{(r,\theta)\in\Psi(\Delta r,\Delta\theta)}|F_1(r,\theta)|^2\sin\theta\,d\theta}{\int_{(r,\theta)\in\Omega}|F_1(r,\theta)|^2\sin\theta\,d\theta} \quad (15)$$

where $\Psi(\Delta r,\Delta\theta)$ is the target area which is the following range-angle sector

$$\Psi(\Delta r,\Delta\theta)=\left\{(r,\theta)/\left|\frac{r-r_0}{R_T}\right|\le\frac{\Delta r}{100};\left|\frac{\theta-\theta_0}{90°}\right|\le\frac{\Delta\theta}{100}\right\} \quad (16)$$

where $R_T=(r_{\max}-r_{\min})/2$, Δr is the percentage in range with reference distance R_T, and $\Delta\theta$ is the percentage in angle with reference angle 90°. Fig. 5 shows the resulting BCE values for the same three previous scenarios. Note that the larger the N, the smaller the obtained target area. However, the proposed FDA-TMA approach achieves BCE values below 10% outside the target areas in all cases. Fig. 5 also plots the BCE obtained with conventional phased arrays, which is constant with respect to the range because conventional phased arrays do not have range focusing capabilities. Notice that the impact of Δf_n on the dot-shaped pattern is on the trade-off BCE versus HPBW, whereas that of D_n is on the range-angle beamsteering.

V. Conclusions

We have presented a combined TMA-FDA innovative method for antenna array beamforming. Without using VPSs, our approach provides quasi-static spatial focusing under certain conditions with a TMA efficiency over 94% and a flexible FDA design employing Kaiser windows to handle the trade-off between BCE and HPBW without any further optimization.

REFERENCES

[1] P. Antonik, M. C. Wicks, H. D. Griffiths, and C. J. Baker, "Frequency diverse array radars," in *2006 IEEE Conference on Radar*, 2006, pp. 3 pp.–.

[2] M. Secmen, S. Demir, A. Hizal, and T. Eker, "Frequency diverse array antenna with periodic time modulated pattern in range and angle," in *2007 IEEE Radar Conference*, 2007, pp. 427–430.

[3] W. Wang, H. C. So, and A. Farina, "An overview on time/frequency modulated array processing," *IEEE Journal of Selected Topics in Signal Processing*, vol. 11, no. 2, pp. 228–246, 2017.

[4] W. Wang, H. C. So, and H. Shao, "Nonuniform frequency diverse array for range-angle imaging of targets," *IEEE Sensors Journal*, vol. 14, no. 8, pp. 2469–2476, 2014.

[5] W. Khan, I. M. Qureshi, and S. Saeed, "Frequency diverse array radar with logarithmically increasing frequency offset," *IEEE Antennas and Wireless Propagation Letters*, vol. 14, pp. 499–502, 2015.

[6] H. Shao, J. Dai, J. Xiong, H. Chen, and W. Wang, "Dot-shaped range-angle beampattern synthesis for frequency diverse array," *IEEE Antennas and Wireless Propagation Letters*, vol. 15, pp. 1703–1706, 2016.

[7] J. Xiong, W. Wang, H. Shao, and H. Chen, "Frequency diverse array transmit beampattern optimization with genetic algorithm," *IEEE Antennas and Wireless Propagation Letters*, vol. 16, pp. 469–472, 2017.

[8] A. Basit, I. M. Qureshi, W. Khan, S. u. Rehman, and M. M. Khan, "Beam pattern synthesis for an fda radar with hamming window-based nonuniform frequency offset," *IEEE Antennas and Wireless Propagation Letters*, vol. 16, pp. 2283–2286, 2017.

[9] A. Yao, W. Wu, and D. Fang, "Frequency diverse array antenna using time-modulated optimized frequency offset to obtain time-invariant spatial fine focusing beampattern," *IEEE Transactions on Antennas and Propagation*, vol. 64, no. 10, pp. 4434–4446, 2016.

[10] ——, "Solutions of time-invariant spatial focusing for multi-targets using time modulated frequency diverse antenna arrays," *IEEE Transactions on Antennas and Propagation*, vol. 65, no. 2, pp. 552–566, 2017.

[11] A. Yao, P. Rocca, W. Wu, A. Massa, and D. Fang, "Synthesis of time-modulated frequency diverse arrays for short-range multi-focusing," *IEEE Journal of Selected Topics in Signal Processing*, vol. 11, no. 2, pp. 282–294, 2017.

[12] A. Yao, P. Rocca, W. Wu, and A. Massa, "On the design of frequency diverse arrays for wireless power transmission," in *2017 11th European Conference on Antennas and Propagation (EUCAP)*, 2017, pp. 900–903.

[13] M. Fartookzadeh, "Comments on "frequency diverse array antenna using time-modulated optimized frequency offset to obtain time-invariant spatial fine focusing beampattern"," *IEEE Transactions on Antennas and Propagation*, vol. 68, no. 2, pp. 1211–1212, 2020.

[14] W. Wu and D. Fang, "Reply to comments on "frequency diverse array antenna using time-modulated optimized frequency offset to obtain time-invariant spatial fine focusing beampattern"," *IEEE Transactions on Antennas and Propagation*, vol. 68, no. 2, pp. 1213–1213, 2020.

[15] R. Maneiro-Catoira, J. A. García-Naya, J. C. Brégains, and L. Castedo, "Multibeam single-sideband time-modulated arrays," *IEEE Access*, vol. 8, pp. 151 976–151 989, 2020.

[16] J. Bregains, J. Fondevila-Gomez, G. Franceschetti, and F. Ares, "Signal radiation and power losses of time-modulated arrays," *IEEE Transactions on Antennas and Propagation*, vol. 56, no. 6, pp. 1799–1804, 2008.

[17] R. Maneiro-Catoira, J. Brégains, J. A. García-Naya, and L. Castedo, "Time-modulated phased array controlled with nonideal bipolar squared periodic sequences," *IEEE Antennas Wireless Propag. Lett.*, vol. 18, no. 2, pp. 407–411, 2019.

[18] K. Prabhu, *Window Functions and Their Applications in Signal Processing (1st ed.)*. CRC Press, 2014.

[19] Y. Xu, X. Shi, J. Xu, and P. Li, "Range-angle-dependent beamforming of pulsed frequency diverse array," *IEEE Transactions on Antennas and Propagation*, vol. 63, no. 7, pp. 3262–3267, 2015.

[20] G. Bogdan, K. Godziszewski, Y. Yashchyshyn, C. H. Kim, and S. B. Hyun, "Time-modulated antenna array for real-time adaptation in wideband wireless systems—part i: Design and characterization," *IEEE Transactions on Antennas and Propagation*, vol. 68, no. 10, pp. 6964–6972, 2020.

[21] A. Yao, P. Rocca, W. Wu, and A. Massa, "On the design of frequency diverse arrays for wireless power transmission," in *2017 11th European Conference on Antennas and Propagation (EUCAP)*, 2017, pp. 900–903.